Hindawi Publishing Corporation
Advances in Acoustics and Vibration
Volume 2016, Article ID 8076108, 7 pages
http://dx.doi.org/10.1155/2016/8076108

Research Article

Generation of Hydroacoustic Waves by an Oscillating Ice Block in Arctic Zones

Usama Kadri

Department of Mathematics, Massachusetts Institute of Technology, Cambridge, MA 02139, USA

Correspondence should be addressed to Usama Kadri; ukadri@mit.edu

Received 2 April 2016; Revised 25 June 2016; Accepted 10 July 2016

Academic Editor: Luc Gaudiller

The time harmonic problem of propagating hydroacoustic waves generated in the ocean by a vertically oscillating ice block in arctic zones is discussed. The generated acoustic modes can result in orbital displacements of fluid parcels sufficiently high that may contribute to deep ocean currents and circulation. This mechanism adds to current efforts for explaining ocean circulation from a snowball earth Neoproterozoic Era to greenhouse earth arctic conditions and raises a challenge as the extent of ice blocks shrinks towards an ice-free sea. Surprisingly, unlike the free-surface setting, here it is found that the higher acoustic modes exhibit a larger contribution.

1. Introduction

The majority of research on ocean circulation neglects the compressibility of water, which is mostly justified. However, it is well known that considering the slight compressibility of water may give rise to compression-type waves [1], known as hydroacoustic waves, or acoustic-gravity waves (under free-surface conditions); see also [2]. It has been shown recently that these waves may contribute to deep ocean currents and circulation [3], as they are continuously generated in the ocean by wind-wave interactions [4, 5], interaction of nearly opposing waves [1, 6–10], and submarine earthquakes [2].

To our knowledge, the vast majority of literature related to this type of waves considers a free-surface boundary condition. As a result, the first mode (often referred to as the zeroth mode) is a surface gravity mode, and its evanescent compartments turn into progressive acoustic modes above a certain cut-off frequency [2]. However, in the case of a rigid boundary replacing the free-surface, propagating and trapped acoustic modes might behave differently as elegantly presented by [11]. In this paper we limit our study to the generation of progressive acoustic modes, by an oscillating block of horizontal ice sheet, and their propagation is confined by horizontal rigid boundaries: the sea floor at the bottom and ice sheets at the top. Obviously, under these conditions and neglecting the elasticity of the boundaries, there can be no gravity surface mode, and all energy is transferred to the acoustic modes. Thus, studying such conditions sheds light on wave energy transfer, as well as water transportation and circulation in confined seas. Here, we present results relevant to arctic zones, from a Neoproterozoic Era [12] to current arctic zones conditions. Oscillations of large ice blocks may be triggered by atmospheric and ocean currents [13], localised wind storms, ice quakes, or other violent geophysical processes.

2. Theoretical Analysis

2.1. Assumptions and Governing Equation. The system considered here is two-dimensional Cartesian coordinates (x, z) with the origin in the midpoint of the ice block; the x-axis is horizontally parallel to the ice sheet (and sea floor), and the z-axis is vertically upwards as shown in Figure 1. The ocean has a constant depth h. The ice block, assumed infinitely long with a total width of $2b$, is oscillating vertically at the angular frequency ω and a small amplitude ζ_0 such that the displacement of the ice block is given by

$$\zeta(x,t) = \zeta_0 \mathscr{H}\left(b^2 - x^2\right) \exp(\mathrm{i}\omega t), \tag{1}$$

where t denotes time, $\mathscr{H}$ is the Heaviside step function, and $\mathrm{i} \equiv \sqrt{-1}$.

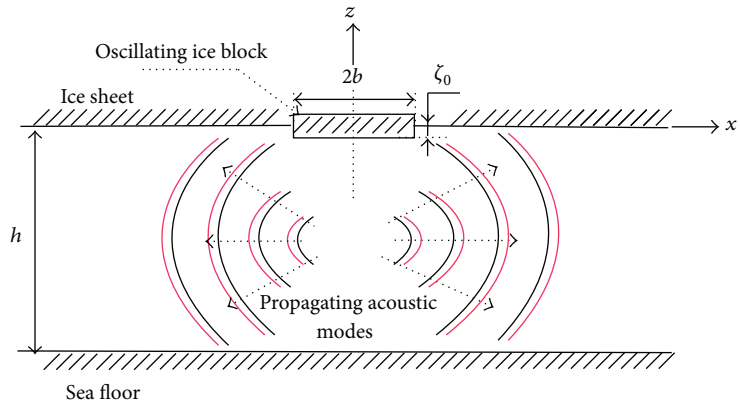

Figure 1: Schematic representation of the flow domain.

The governing equation is the standard two-dimensional compressible wave equation [14, 15]. Applying the appropriate boundary conditions and using standard techniques the following horizontal and vertical fluid velocities, u_n and w_n, induced by the nth acoustic mode can then be derived (see the Appendix):

$$u_n(x,z,t) = \begin{cases} \mp 2i\zeta_0 \dfrac{\mu_n \cos\left[\mu_n (z+h)\right] \sin\left(k_n b\right) \exp\left[-\mathrm{i}\left(k_n x - \omega t - \pi/2\right)\right]}{k_n \cos\left(\mu_n h\right)}, & |x| > b, \\ -2i\zeta_0 \dfrac{\mu_n \cos\left[\mu_n (z+h)\right] \cos\left(k_n b\right) \exp\left[-\mathrm{i}\left(k_n |x| - \omega t\right)\right]}{k_n \cos\left(\mu_n h\right)}, & |x| < b, \end{cases} \tag{2}$$

$$w_n(x,z,t) = \begin{cases} \mp 2\zeta_0 \dfrac{\mu_n^2 \sin\left[\mu_n (z+h)\right] \sin\left(k_n b\right) \exp\left[-\mathrm{i}\left(k_n x - \omega t - \pi/2\right)\right]}{k_n^2 \cos\left(\mu_n h\right)}, & |x| > b, \\ -2\zeta_0 \dfrac{\mu_n^2 \cos\left[\mu_n (z+h)\right] \sin\left(k_n b\right) \exp\left[-\mathrm{i}\left(k_n |x| - \omega t\right)\right]}{k_n^2 \cos\left(\mu_n h\right)}, & |x| < b, \end{cases} \tag{3}$$

where μ_n is the eigenvalue and k_n is the horizontal wavenumber.

3. Results and Discussion

3.1. Displacements. In order to obtain the horizontal and vertical particle displacement components $(X_n; Z_n)$ we integrate (2) with respect to time, so that, for $|x| > b$, we can write $X_n = A\sin(k_n x - \omega t)$ and $Z_n = B\cos(k_n x - \omega t)$, where $(X_n/A)^2 + (Z_n/B)^2 = 1$ is the equation of an ellipse with a horizontal semiaxis A and a vertical semiaxis B given by

$$A = \pm\frac{2\zeta_0}{\omega}\frac{\mu_n \cos\left[\mu_n (z+h)\right] \sin\left(k_n b\right)}{k_n \cos\left(\mu_n h\right)};$$
$$B = \mp\frac{2\zeta_0}{\omega}\frac{\mu_n^2 \sin\left[\mu_n (z+h)\right] \sin\left(k_n b\right)}{k_n^2 \cos\left(\mu_n h\right)}. \tag{4}$$

The orbital behaviours of the acoustic modes are periodic with depth as shown in Figure 2, with $n/2$ wavelengths fitting the depth h, in opposition to the free-surface setting in which $(2n-1)/4$ wavelengths fit the depth [3, 16]. For the numerical calculations we considered a speed of sound $c = 1500\,\mathrm{m/s}$, $h = 4500\,\mathrm{m}$, $b = 10^4\,\mathrm{m}$, $\zeta_0 = 1\,\mathrm{m}$, and $\omega = 5\,\mathrm{rad/s}$. With the current setting, the obtained displacements correspond to horizontal and vertical velocities reaching up to tens of centimetres per second for the first mode, which is comparable to those obtained by an equivalent underwater earthquake with a free surface [2, 3]. However, a distinguishable result here is that the leading mode is not necessarily the first acoustic, but the highest acoustic mode (which can be obtained from (A.9)) given by

$$N_{\max} = \left\lfloor \frac{\omega h}{\pi c} \right\rfloor, \tag{5}$$

where the special brackets represent the floor function. For the case of $n = N_{\max}$, the displacements and velocities may become one order of magnitude larger than those of the first acoustic mode, $n = 1$, and thus, unlike the free-surface problem, all progressive acoustic modes have to be considered.

Note that the choice of $\zeta_0 = 1\,\mathrm{m}$ far exceeds observed amplitudes of oscillating sea-ice blocks in the late Common Era [17]. Nevertheless this choice allows a proper comparison with the free-surface underwater earthquake problem [2] emphasising the importance of the higher modes and directly reflects on two actual scenarios. The first scenario describes an underwater earthquake in the arctic ocean, in particular

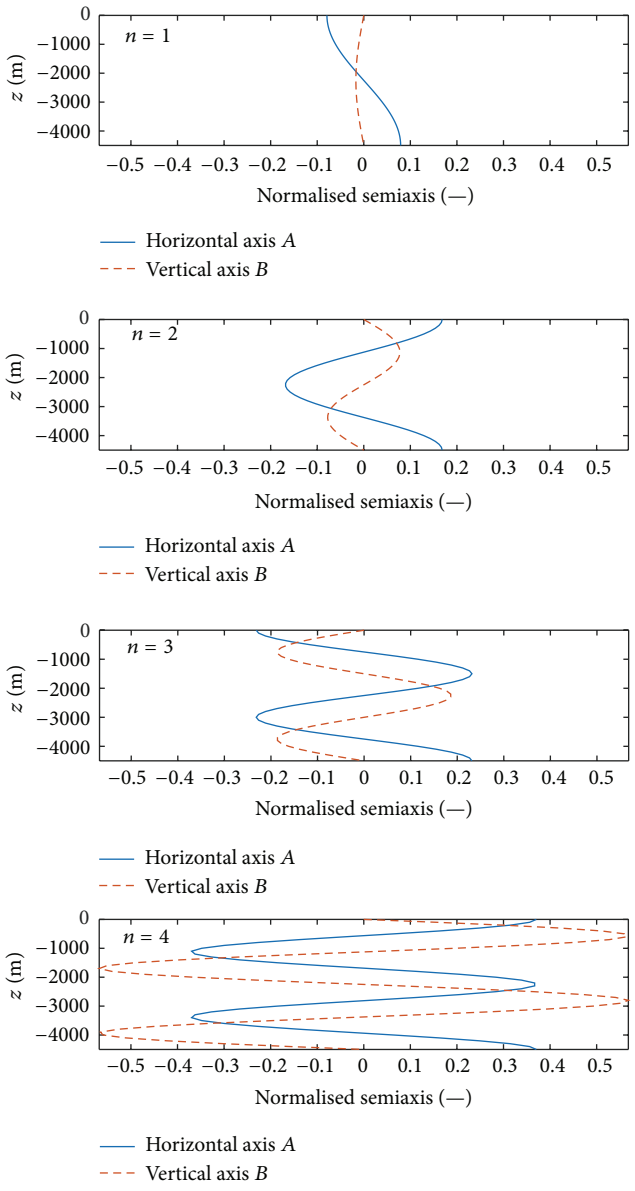

FIGURE 2: Semiaxis of water parcels for acoustic modes, from top to bottom: $n = 1, 2, 3, 4$; $h = 4500$ m, $c = 1500$ m/s, $b = 10^4$ m, $\zeta_0 = 1$ m, and $\omega = 5$ rad/s.

in winter if the sea surface is completely frozen. Recall that in the absence of gravity and elasticity, while the mathematical solution in hand is valid for a rigid sea floor and an oscillating ice block at the surface (oscillating ice block problem), it is equally valid for the setting with a rigid frozen surface and an oscillating sea floor block at the bottom (e.g., earthquake in the arctic ocean). The second scenario considers the snowball earth Neoproterozoic Era, where sea-ice thickness might have exceeded a kilometre. Under such conditions, ice quakes and other violent geophysical phenomena could have caused oscillations with amplitudes that are comparable with the chosen $\zeta_0 = 1$ m. Further qualitative analysis through the different climate eras is given in the last section.

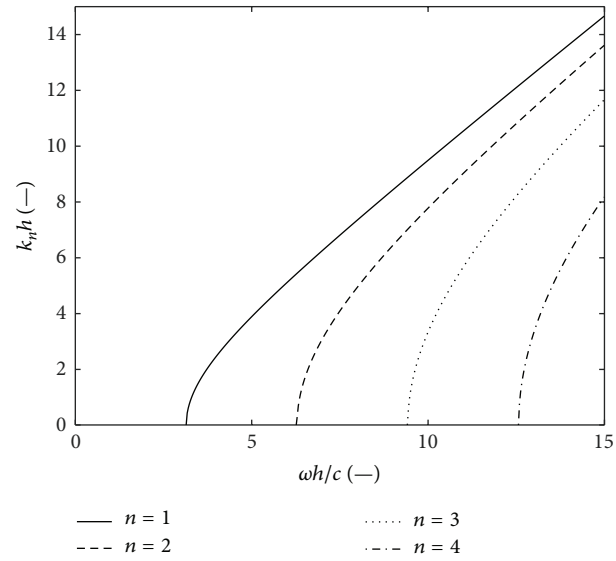

FIGURE 3: Dispersion of modes; $h = 4500$ m and $c = 1500$ m/s.

3.2. Dispersion Relation. The dispersion relation is given in nondimensional form by

$$\mu_n k_n h^2 \sinh(\mu_n h) = 0. \tag{6}$$

For the incompressible case $\omega h/c \to 0$, and therefore $\mu_n \to k_n$. In this case there is no nontrivial solution, and no waves are formed. For the compressible case, the wavenumber of the acoustic mode is given by

$$k_n h = \left(\frac{\omega^2 h^2}{c^2} - n^2\pi^2\right)^{1/2}, \quad n = 1, \ldots, N_{\max}, \tag{7}$$

where $N_{\max}$ is the maximum number of progressive acoustic modes. Thus, the cut-off frequency for each mode is given by $\omega_c = n\pi c/h$, so that, at a given depth and relatively low frequencies $\omega < \omega_c$, only evanescent modes can exist, whereas when $\omega > \omega_c$ there should be at least one nonevanescent acoustic mode. For the case of $h = 4500$ m the cut-off frequency is $\omega_c = \pi/3$. The dispersion relations of $k_n h$ versus $\omega h/c$ are shown in Figure 3. It is easy to show that the group velocities, defined as $c_g = (\mathrm{d}\omega/\mathrm{d}k_n)$, differ from one mode to another though all tend to the sound speed c if the normalised frequency $(\omega h/c)$ is large enough. These can be obtained from the slopes of the dispersion relations presented in Figure 3.

3.3. Energy Aspects. The total wave energy is composed of two parts: kinetic and elastic potential; with the absence of a free surface there is no gravity potential energy. Following similar steps as given by [2] we obtain an expression for the kinetic energy per unit volume:

$$E_{\kappa,n} = \frac{1}{2}\rho\zeta_0^2 \frac{\omega^4 \mu_n \left[\sin(2\mu_n h) + 2\mu_n h\right] \sin^2(k_n b)}{hc^2 k_n^4 \cos^2(\mu_n h)} \tag{8}$$

and the elastic energy is $E_{\epsilon,n} = E_{\kappa,n}/4$. Above the cut-off frequency the oscillation of the ice block results in energy "transfer" to the corresponding acoustic mode/modes (Figure 4).

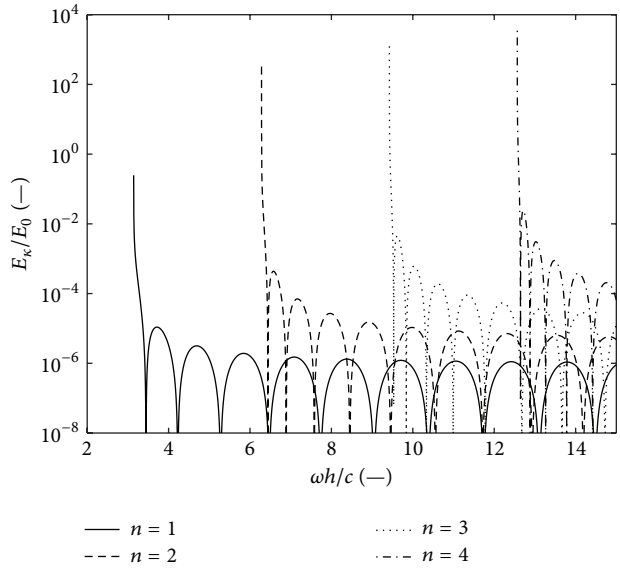

FIGURE 4: Kinetic energy versus frequency; $h = 4500$ m, $c = 1500$ m/s, $b = 10^4$ m, and $\zeta_0 = 1$ m.

However, below the cut-off frequency, the fluid becomes incompressible and no energy transfer occurs. With regard to this point it is worth noting that below the cut-off frequency the stratification of the ocean or the elasticity of the sea floor and ice sheets, which was neglected in the presented analysis, might become important [18]. Considering stratification may give rise to internal gravity waves that are believed to be a major driver of deep ocean mixing [19]. On the other hand, considering the elasticity of the boundaries, it is anticipated that oscillations below the cut-off frequency would give rise to a Scholte-type modes that propagate through both interfaces, with the sea floor and with the ice sheet [20]. Other types of trapped modes are discussed in detail by [11].

It is also notable that the fact that the higher acoustic modes have a larger contribution on water transport compared to the lower modes suggests that the flow field would become temporally and spatially nonuniform, if stratification is considered, as also found in observations [21–25]. Nevertheless, stratification or consequently variations in the speed of sound do not practically have a direct effect on the fluid motion induced by a hydroacoustic wave, whose group velocity remains almost unaltered. Hence, stratification is not considered in the current analysis, though a numeric comparison with the effects of internal gravity waves due to stratification is briefly presented in the following section.

3.4. From Snowball to Greenhouse Earth. The water motion in the ocean plays a prominent role in distributing heat, originated from solar radiation or hydrothermal activities, around the globe. In free-surface open seas, ocean water results in humidification and increasing the temperature of the surrounding air, which in turn forms storms and rain. Without currents and underwater streams localised temperatures become more severe leading to extreme global weather. Hence, water motion in the ocean acts as a global climate regulator.

The flow generated by the motion of the ice block is equivalent to the superposed flow by two line sources located at the edges of the ice block $x = \pm b$. Such superposition can be either destructive or constructive, resulting in various peak velocities, as given qualitatively in Figure 5. A minimal flow field is created when the oscillating ice block has a width $2b$ multiples of a wavelength for each acoustic mode; that is, $2b = NL_n$, where $L_n = 2\pi/k_n$ is the wavelength, and $N = 1, 2, 3, \ldots$. On the other hand, a maximal flow field is induced when $2b = L_n(N - 1/2)$. Thus, the mutual existence of multiple acoustic modes is expected to create regions of minimal and maximal peak velocities as confirmed by Figure 6. It is worth mentioning here that deep ocean currents induced by internal gravity waves can travel at speeds varying from 0.02 to 0.1 m/s, whereas surface currents (that do not exist in snowball earth) can travel at speeds as high as 2.5 m/s. Thus, from Figure 6, it is clear that internal gravity waves become more important in a greenhouse earth, as opposed to hydroacoustic waves, keeping in mind that the latter, despite the lower induced peak velocities, would still span the entire depth.

It is believed that during the Neoproterozoic Era the earth was fully covered by snow, with ice blocks that extended over hundreds of metres thickness [12, 26]. It was suggested by [26] that during the Neoproterozoic Era ice could have extended to hundreds or thousands of kilometres, with sea ice that could have covered up to 14×10^6 km^2 of the Arctic Ocean during winter [27]. Thus, ice blocks could have been of the scale of tectonic plates [26], with similar vertical displacements, that probably exceeded our choice of $\zeta_0 = 1$ m, in particular with violent geophysical events that characterised that period. In this regard, it is also expected that multiple extremely long period oscillations could have formed high amplitude progressive waves causing circulations at velocity magnitudes of centimetres per second that are many orders of magnitudes higher than those from the suggested geothermal mechanism (i.e., micrometers per second) by [12] for that era. Here, it is also notable that, due to the differences in scales and distribution of events, the significance of two mechanisms could be decoupled in the space-time domain.

In the eighties of the last century the mean extent of the ice covering the arctic ocean had shrank to a value of less than 16 million squared kilometres, decreasing at a rate of 3% per decade [13]. Clearly, the ice pack thickness was dramatically reduced, and as the sea ice thins and shrinks further, it is expected that ice block oscillations will take place at relatively smaller areas and have less impact. In addition, recent observations suggest that, under current conditions, ice block oscillation amplitude may not exceed a few millimetres [17], producing a weak pressure signature on fluid parcels residing through the water column. Due to the different nature of waves radiated from ice-sheet movements, which is relatively a new scientific discipline, or even near sea glaciers, the available high quality data goes back to a few years only. It is well known that hundreds of ice quakes occur annually in localised regions, some of which are related to glacial-sea interface and have magnitudes that may exceed 5 [28]. At such discontinuous space-time interaction events, any impact is expected to be localised, and the contribution

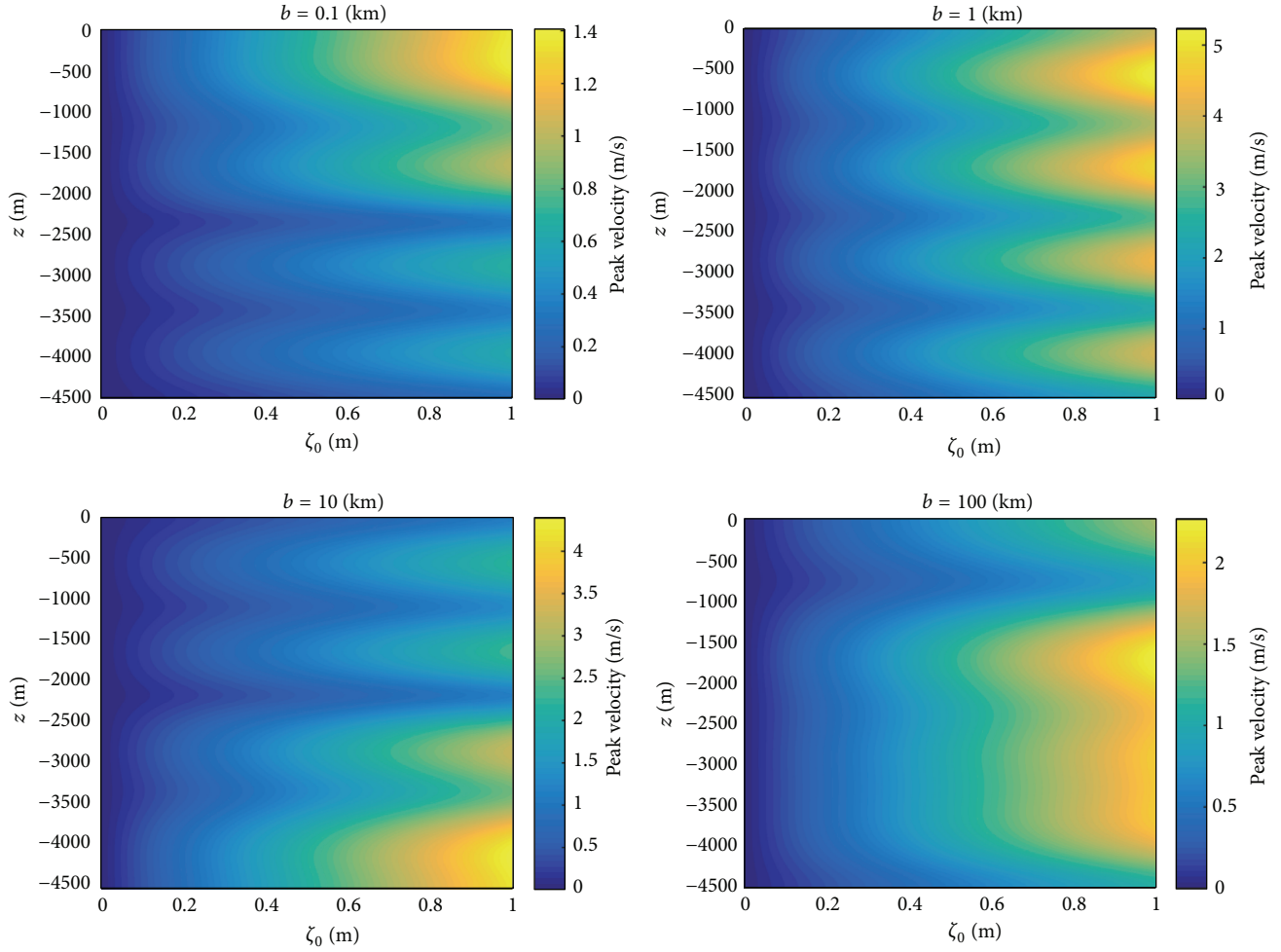

FIGURE 5: Peak velocities induced by four different oscillating ice blocks, $b = 0.1, 1, 10$, and 100 km, with various amplitudes $0 < \zeta_0 < 1$; $h = 4500$ m and $c = 1500$ m/s.

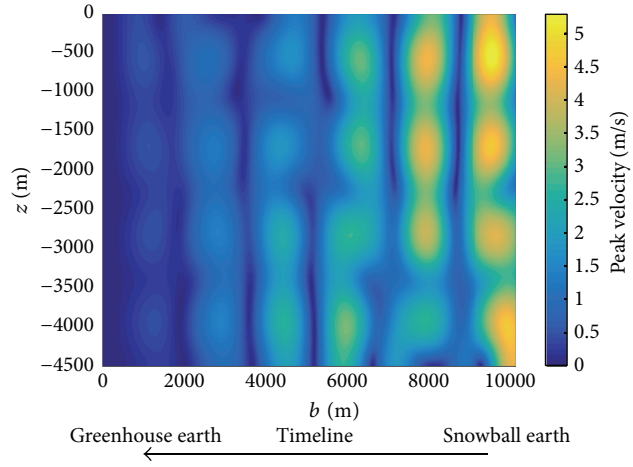

FIGURE 6: Peak velocities from various ice block widths representing timeline from snowball to greenhouse earth, from right to left. The amplitude $\zeta_0 = 0.0001b$; $h = 4500$ m and $c = 1500$ m/s.

to water circulation becomes far less efficient, compared to snowball earth conditions. A qualitative demonstration of the change of impact of the ice block oscillations from snowball to greenhouse earth is given in Figure 6 where the x-axis represents the timeline, from right to left.

The Arctic Ocean is relatively poor in marine life, in general, and in plants, in particular. Although Phytoplankton is amongst the few marine plants in the Arctic Ocean, they are essential for sustaining a healthy ocean. Phytoplankton feed on nutrients from currents and water transport. As the greenhouse effect sustains and more areas of ice packs shrink and thin, one can expect a decrease in the generation of acoustic, by the present mechanism. On the other hand, if the sea becomes completely ice free [29], that gives rise to local formation of acoustic by interacting surface gravity waves [7, 9, 10]. The transition between the different mechanisms would possibly disturb global current patterns. Such disturbance is expected to affect nutrients transport and Phytoplankton population and potentially cause severe climate changes [30, 31], which is left for future work.

Appendix

Derivation of the Displacements

The governing equation is the standard two-dimensional compressible wave equation [14, 15]:

$$\varphi_{tt} - c^2\nabla^2\varphi = 0, \quad -h \le z \le 0, \tag{A.1}$$

where φ is the velocity potential.

The upper boundary condition is given by

$$\varphi_z = \zeta_t, \quad z = 0, \tag{A.2}$$

and the bottom boundary condition is simply

$$\varphi_z = 0, \quad z = -h. \tag{A.3}$$

Since here we only consider time harmonic problems we can write

$$\varphi(x, z, t) = f(x, z)\exp(\mathrm{i}\omega t). \tag{A.4}$$

Substituting (A.4) into (A.1), (A.2), and (A.3) and making use of (1) give

$$\begin{aligned} \nabla^2 f + \frac{\omega^2}{c^2} f = 0, \quad & -h \le z \le 0, \\ f_z = \zeta_0 \mathscr{H}\left(b^2 - x^2\right), \quad & z = 0, \\ f_z = 0, \quad & z = -h. \end{aligned} \tag{A.5}$$

In the space domain the upper boundary condition is inhomogeneous. To overcome this difficulty we apply a Fourier transformation to the wavenumber domain, where $F(w, z)$ is the transform of $f(x, z)$, defined by

$$F(w, z) = \int_{-\infty}^{\infty} \exp(-\mathrm{i}wx)\, f(x, z)\, \mathrm{d}x \tag{A.6}$$

and the inverse transform, defined by

$$f(x, z) = \frac{1}{2\pi}\int_{-\infty}^{\infty} \exp(\mathrm{i}wx)\, F(w, z)\, \mathrm{d}x. \tag{A.7}$$

Defining $w = k + \mathrm{i}\lambda$, where k and λ are real positive numbers, the eigenvalues can be written as

$$w = 0, \pm k_s, \pm k_n, \pm \mathrm{i}\lambda_n, \quad n = 1, 2, \ldots, \tag{A.8}$$

where

$$\begin{aligned} k_s &= \frac{\omega}{c}; \\ k_n &= \left(k_s^2 - \mu_n^2\right)^{1/2}, \quad \mu_n < k_s; \\ \lambda_n &= \left(\mu_n^2 - k_s^2\right)^{1/2}, \quad \mu_n > k_s. \end{aligned} \tag{A.9}$$

Using standard techniques as given by [2], in which a Fourier transform is applied over the horizontal axis, we obtain an expression for $f(x, z)$. For the range $|x| > b$ we write

$$\begin{aligned} f(x, z) &= \pm 2\zeta_0 \left\{ \sum_{n=1}^{N} \frac{\mu_n \cos\left[\mu_n (z + h)\right] \sin\left(k_n b\right) \exp\left[-\mathrm{i}\left(k_n x - \pi/2\right)\right]}{k_n^2 \cos\left(\mu_n h\right)} \right. \\ &\quad \left. \mp \sum_{n=N+1}^{\infty} \frac{\mu_n \cos\left[\mu_n (z + h)\right] \sinh\left(\lambda_n b\right) \exp\left(\mp \mathrm{i}\lambda_n x\right)}{\lambda_n^2 \cos\left(\mu_n h\right)} \right\}, \end{aligned} \tag{A.10}$$

where the upper signs of $(\pm)$ and $(\mp)$ in (A.10) are for $x > b$ and the lower ones are for $x < b$. On the other hand, for the range $|x| < b$, we write

$$\begin{aligned} f(x, z) &= 2\zeta_0 \left\{ \sum_{n=1}^{N} \frac{\mu_n \cos\left[\mu_n (z + h)\right] \cos\left(k_n b\right) \exp\left(-\mathrm{i}k_n |x|\right)}{k_n^2 \cos\left(\mu_n h\right)} \right. \\ &\quad - \sum_{n=N+1}^{\infty} \frac{\mu_n \cos\left[\mu_n (z + h)\right] \cosh\left(\lambda_n x\right) \exp\left(-\lambda_n b\right)}{\lambda_n^2 \cos\left(\mu_n h\right)} \\ &\quad \left. + \frac{\cos\left[k_s (z + h)\right]}{k_s \sin\left(k_s h\right)} \right\}. \end{aligned} \tag{A.11}$$

The first terms of right-hand side of (A.10) and (A.11) represent the acoustic modes, whereas the second terms represent the evanescent acoustic modes, which exponentially decay from the source and thus will not be considered in the sequel. The third term of (A.11) represents the surge mode which exists only below the oscillating ice block at $|x| < b$.

Ignoring the evanescent and surge terms in (A.10) and (A.11), substituting into the potential equation (A.4), and differentiating with respect to x and z give the horizontal and vertical velocities, respectively.

Competing Interests

The author declares that there are no competing interests.

Acknowledgments

The author thanks Carl Wunsch for raising the question that resulted in this paper and Raffaele Ferrari for useful discussions.

References

[1] M. S. Longuet-Higgins, "A theory of the origin of microseisms," *Philosophical Transactions of the Royal Society of London. Series A. Mathematical and Physical Sciences*, vol. 243, pp. 1–35, 1950.

[2] T. Yamamoto, "Gravity waves and acoustic waves generated by submarine earthquakes," *International Journal of Soil Dynamics and Earthquake Engineering*, vol. 1, no. 2, pp. 75–82, 1982.

[3] U. Kadri, "Deep ocean water transport by acoustic-gravity waves," *Journal of Geophysical Research: Oceans*, vol. 119, no. 11, pp. 7925–7930, 2014.

[4] F. Ardhuin, T. Lavanant, M. Obrebski et al., "A numerical model for ocean ultra-low frequency noise: wave-generated acoustic-gravity and Rayleigh modes," *The Journal of the Acoustical Society of America*, vol. 134, no. 4, pp. 3242–3259, 2013.

[5] S. Kedar, M. Longuet-Higgins, F. Webb, N. Graham, R. Clayton, and C. Jones, "The origin of deep ocean microseisms in the North Atlantic Ocean," *Proceedings of the Royal Society A: Mathematical, Physical and Engineering Sciences*, vol. 464, no. 2091, pp. 777–793, 2008.

[6] W. Farrell and W. Munk, "Booms and busts in the deep," *Journal of Physical Oceanography*, vol. 40, no. 9, 2010.

[7] U. Kadri, "Wave motion in a heavy compressible fluid: revisited," *European Journal of Mechanics B. Fluids*, vol. 49, pp. 50–57, 2015.

[8] U. Kadri, "Triad resonance between a surface-gravity wave and two high frequency hydro-acoustic waves," *European Journal of Mechanics B: Fluids*, vol. 55, no. 1, pp. 157–161, 2016.

[9] U. Kadri and T. R. Akylas, "On resonant triad interactions of acoustic—gravity waves," *Journal of Fluid Mechanics*, vol. 788, article R1, 12 pages, 2016.

[10] U. Kadri and M. Stiassnie, "Generation of an acoustic-gravity wave by two gravity waves, and their subsequent mutual interaction," *Journal of Fluid Mechanics*, vol. 735, article R6, 9 pages, 2013.

[11] C. M. Linton and P. McIver, "Embedded trapped modes in water waves and acoustics," *Wave Motion*, vol. 45, no. 1-2, pp. 16–29, 2007.

[12] Y. Ashkenazy, H. Gildor, M. Losch, and E. Tziperman, "Ocean circulation under globally glaciated snowball earth conditions: steady-state solutions," *Journal of Physical Oceanography*, vol. 44, no. 1, pp. 24–43, 2014.

[13] C. L. Parkinson, D. J. Cavalieri, P. Gloersen, H. J. Zwally, and J. C. Comiso, "Arctic sea ice extents, areas, and trends, 1978–1996," *Journal of Geophysical Research: Oceans*, vol. 104, no. 9, pp. 20837–20856, 1999.

[14] R. Stoneley, "The effect of the ocean on Rayleigh waves," *Geophysical Journal International*, vol. 1, pp. 349–356, 1926.

[15] H. Lamb, *Hydrodynamics*, Cambridge University Press, Cambridge, UK, 6th edition, 1932.

[16] F. B. Jensen, W. A. Kuperman, M. B. Porter, and H. Schmidt, *Computational Ocean Acoustics*, Springer, New York, NY, USA, 2011.

[17] D. R. MacAyeal, E. A. Okal, R. C. Aster, and J. N. Bassis, "Seismic and hydroacoustic tremor generated by colliding Icebergs," *Journal of Geophysical Research: Earth Surface*, vol. 113, no. 3, 2008.

[18] E. Eyov, A. Klar, U. Kadri, and M. Stiassnie, "Progressive waves in a compressible-ocean with an elastic bottom," *Wave Motion*, vol. 50, no. 5, pp. 929–939, 2013.

[19] R. Ferrari and C. Wunsch, "Ocean circulation kinetic energy: reservoirs, sources, and sinks," *Annual Review of Fluid Mechanics*, vol. 41, no. 1, pp. 253–282, 2009.

[20] P. D. Bromirski and R. A. Stephen, "Response of the ross ice shelf, antarctica, to ocean gravity-wave forcing," *Annals of Glaciology*, vol. 53, no. 60, pp. 163–172, 2012.

[21] E. A. D'Asaro and J. H. Morison, "Internal waves and mixing in the Arctic Ocean," *Deep Sea Research Part A: Oceanographic Research Papers*, vol. 39, no. 2, pp. S459–S484, 1992.

[22] C. Halle and R. Pinkel, "Internal wave variability in the Beaufort Sea during the winter of 1993/1994," *Journal of Geophysical Research C: Oceans*, vol. 108, no. 7, article 3210, 2003.

[23] M. D. Levine, C. A. Paulson, and J. H. Morison, "Internal waves in the arctic ocean: comparison with lower-latitude observations," *Journal of Physical Oceanography*, vol. 15, no. 6, pp. 800–809, 1985.

[24] R. Pinkel, "Near-inertial wave propagation in the western Arctic," *Journal of Physical Oceanography*, vol. 35, no. 5, pp. 645–665, 2005.

[25] A. J. Plueddemann, "Internal wave observations from the Arctic environmental drifting buoy," *Journal of Geophysical Research: Oceans*, vol. 97, no. 8, pp. 12619–12638, 1992.

[26] P. F. Hoffman, A. J. Kaufman, G. P. Halverson, and D. P. Schrag, "A neoproterozoic snowball earth," *Science*, vol. 281, no. 5381, pp. 1342–1346, 1998.

[27] J. Weiss, "Scaling of fracture and faulting of ice on earth," *Surveys in Geophysics*, vol. 24, no. 2, pp. 185–227, 2003.

[28] I. Joughin, "Greenland rumbles louder as glaciers accelerate," *Science*, vol. 311, no. 5768, pp. 1719–1720, 2006.

[29] J. E. Overland and M. Wang, "When will the summer Arctic be nearly sea ice free?" *Geophysical Research Letters*, vol. 40, no. 10, pp. 2097–2101, 2013.

[30] J. O. Sewall and L. C. Sloan, "Disappearing arctic sea ice reduces available water in the american west," *Geophysical Research Letters*, vol. 31, no. 6, Article ID L06209, 2004.

[31] J. A. Francis and S. J. Vavrus, "Evidence linking arctic amplification to extreme weather in mid-latitudes," *Geophysical Research Letters*, vol. 39, no. 6, Article ID L06801, 2012.